

## Photodegradation Efficiency of MIL-53Al on Azo Dyes

**Keywords,** Reactive Azo dyes, metal-organic framework (MIL-53Al), kinetics, photodegradation

### Abstract

Photodegradation of Azo reactive dyes (color index Yellow 145 and Blue 194) under sunlight using metal-organic framework MIL-53(Al) were evaluated. The synthesized material was characterized using FTIR and XRD techniques. The degradation process was assessed using varying amounts of 1.5 g, 1.0 g, and 0.5 g of the catalyst. The percentage degradation for the color index Yellow 145 after 30mins was 44.92 %, 32.84 %, and 16.44 % for 1.5 g, 1.0 g, and 0.5 g and it increased to 96.72 %, 89.34 %, and 82.22 % for 1.5 g, 1.0 g, and 0.5 g respectively after 240 mins of treatment. For the color index Blue 194, the initial 30 mins recorded a percentage reduction of 61.0 %, 38.3 %, and 14.92 % for the masses of 1.5 g, 1.0 g, and 0.5 g respectively and after 240 mins it increased to 92.0 %, 85.47 %, and 82.2 % for the 1.5 g, 1.0 g, and 0.5 g masses respectively. The Pseudo-first-order degradation kinetics color index Yellow 145 recorded  $R^2$  values of 0.9765, 0.9697, and 0.9853 for 1.5 g, 1.0 g, and 0.5 g respectively. The Pseudo-second-order degradation process also recorded  $R^2$  values as 0.9966, 0.9956, and 0.8114 for 1.5 g, 1.0 g, and 0.5 g of MIL-53(Al). The Pseudo-first-order degradation graph for color index Blue 194, has  $R^2$  values of 0.9789, 0.9954, 0.9787 for the 1.5 g, 1.0 g, and 0.5 g of the catalyst used. The Pseudo-second-order degradation kinetics of color index Blue 194 using MIL-53(Al) also recorded  $R^2$  values of 0.9998, 0.9937, and 0.6885 for the 1.5 g, 1.0 g, and 0.5 g mass catalysts.

**Keywords,** Reactive Azo dyes, Metal-organic framework (MIL-53A1), kinetics, photodegradation

## 1.0 Introduction

Industrialization plays an important role in the economic life of every country. Most industrial activities such as petroleum, textile, pharmaceuticals, and hospitality release several volumes of untreated effluent into drains and water bodies. In recent times, research in new methodologies for the treatment of recalcitrant compounds (e.g. dyes, drugs, pesticides, steroids), commonly found in wastewater of industrial and pharmaceutical processes, is a prominent field in engineering and natural sciences [1]. There are a huge number of different types of organic pollutants, including organic dyes, phenols, biphenyls, pesticides, fertilizers, hydrocarbons, plasticizers, detergents, oils, greases, pharmaceuticals, proteins, carbohydrates [2]. One of the main sources of water pollution is largely the wastewater from the textile, paper, or printing industries [3, 4]. Some of the dyes that pollute the environment are azo dyes that are discharged in large quantities, directly in water bodies, characterizing an important way of environmental contamination [5]. The treatment of dye-containing wastewater presents a tremendous challenge for human beings not only because of the still rapidly growing amount of discharge but also as a result of the stable structures of dye molecules which are usually conjugated and render them chemically inert to light, heat, and oxidizing agents, and therefore make it rather difficult to decompose or degrade [6]. Although several methods, such as adsorption, biodegradation, chemical oxidation, coagulation, and flocculation [7-10] have been used for the treatment of dyes, new materials and technologies [11] with high efficiency, wide applicability, economic feasibility, and simplicity of design/operation are still urgently needed to better cope with this increasingly serious pollution issue, especially in some developing countries.

In recent researches, different chemicals and photochemical processes such as electrochemical oxidation [12], thermic plasma [13], Fenton process [14], ozonization [15], photo-Fenton [16], homogenous and heterogeneous photocatalysis [17] have been proposed as alternative degradation technologies for recalcitrant compounds such as Azo dyes. Metal-organic frameworks (MOFs), also known as Porous Coordination Polymers (PCPs) or Porous Coordination Networks (PCNs), are a new class of porous materials consisting of metal ions or clusters and organic linkers [18-20] and because of their tunable structure, porosity, and functionality, they have several applications such as gas storage [19, 21-25], gas separation [26, 27], catalysis [28], sensing [29-32], light-harvesting [33], and optical luminescence [34, 35]. Several metal-organic frameworks have been used to photodegrade industrial dyes from aqueous solutions. Qiu and his research group found that the efficient degradation of methylene blue (MLB) can be achieved under the irradiation of UV or visible light by using MIL-53(Fe) as photocatalyst [36]. A researcher, Xing's and his group recently reported that NNU-36 is a highly efficient heterogeneous photocatalyst for the reduction of aqueous Cr(VI) and degradation of dyes (Rhodamine B: RhB; Rhodamine 6G:R6G, MLB) [37].

Amino-MIL-101(Al) has very high adsorptive capacity for Methyl Orange [38] and nanostructured ZIF-8 on silica microspheres can degrade Methyl Orange due to its surface functionalities ( $-\text{SH}$ ,  $-\text{COOH}$ , and  $-\text{NH}_2$ )

MOFs based on Al-carboxylate coordination chemistry are regarded to be one of the most thermally and chemically stable of such systems [39-41] and it will be very interesting to research photocatalytically active aluminum-based MOFs which are of great practical and scientific importance. Al-based MOFs are stable, highly active, and used as a basic catalyst in a Knoevenagel condensation, to be well-suited for  $\text{CO}_2/\text{CH}_4$  separation [42, 43] to exhibit good adsorption behavior of organic dyes [44, 45] and to be fluorescent sensors for  $\text{Fe}^{3+}$  [46]. It has also been realized that Al-carboxylate-based MOFs have proved to be photo-responsive, and exhibit photocatalytic activity towards RhB degradation and  $\text{CO}_2$  reduction [47, 48]. In this research work, Al-based MOF MIL-53(Al) was synthesized using terephthalic acid and characterized by the X-Ray diffraction, and the Fourier Transform Infrared. The synthesized material was then used to photodegrade some Reactive Azo dyes and the products of the process were assessed. This research is graphically presented below

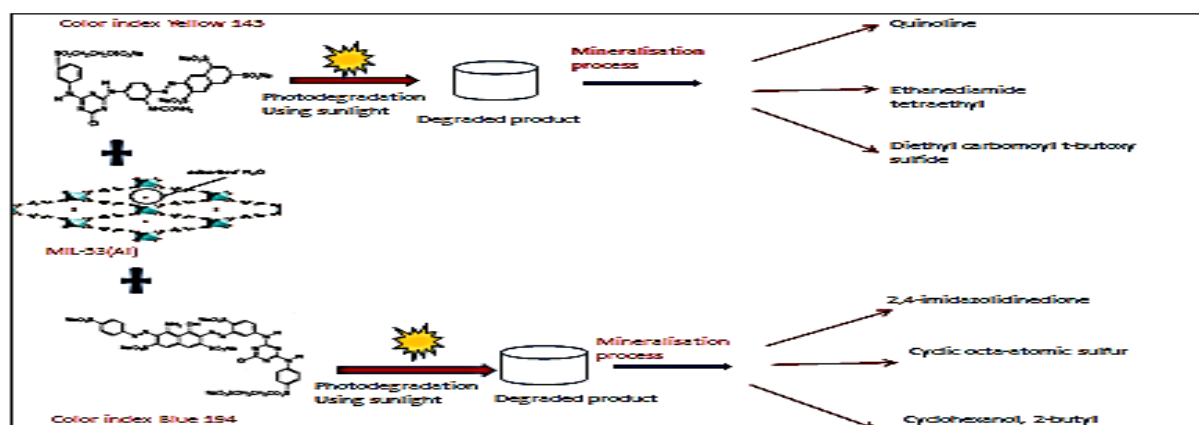


Figure 1 Graphical representation of the research work

Figure 2 and Figure 3 below show the chemical structures of dyes color index Yellow 145 and color index Blue 194, which were used in this research work.

Molecular Formula:  $\text{C}_{28}\text{H}_{20}\text{ClN}_9\text{Na}_4\text{O}_{16}\text{S}_5$   
Colour Index Reactive Yellow 145

Molecular Formula:  $\text{C}_{33}\text{H}_{22}\text{ClN}_{10}\text{Na}_5\text{O}_{19}\text{S}_6$   
Colour Index Reactive Blue 194

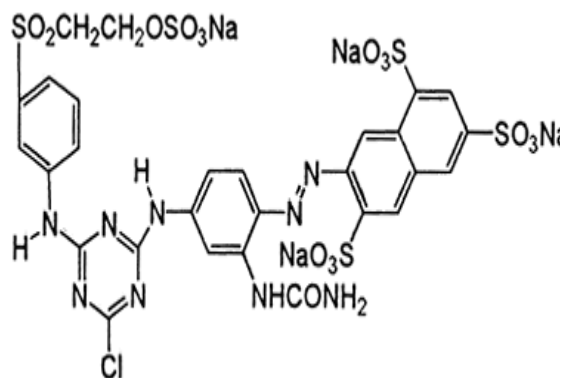


Figure 2: A figure showing the structure of Color Index Yellow 145

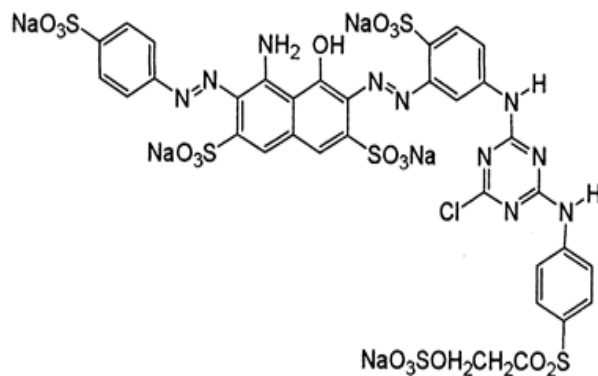


Figure 3: A figure showing the structure of Color Index Blue 194

## 2.0 Experimental

### 2.1 Materials and Methods

The chemicals used are Aluminum nitrate, benzenedicarboxylic acid, N, N-Dimethylformamide, hexane, Acetonitrile, Magnesium hydrate, and deionized water. All reagents were analytical grade and were used without further purification. The equipment used is 100 ml Teflon lined stainless Autoclave, X-ray diffractometer, Fourier Transform Infra-red, and UV-Vis Spectrophotometer (Shimadzu, UV-160A).

### 2.2 Synthesis of MIL-53(Al)

MIL-53(Al) was solvothermally synthesized following a literature procedure by Yan, J., Jiang, S., Ji, S. et al. (2015) [49] where 13.0 g of Aluminum nitrate ( $\text{Al}(\text{NO}_3)_3 \cdot 9\text{H}_2\text{O}$ ) and 2.88g 1,4-benzenedicarboxylic acid ( $\text{H}_2\text{BDC}$ ) were mixed with 50mL deionized water in a 100mL Teflon-lined stainless steel autoclave and then placed in an oven at  $220^\circ\text{C}$  for 72 hours. The autoclave was then removed after the time and allowed to cool. The product was filtered and washed. It was further purified with a solvent extraction method using N, N-Dimethylformamide (DMF) to remove residual  $\text{H}_2\text{BDC}$ . The filtrate was then washed with methanol to remove residual DMF molecules trapped inside the cavities and finally dried at  $80^\circ\text{C}$  for 2 hours.

### 2.3 Characterization of Synthesized MIL-53(Al)

The synthesized material was characterized by the X-Ray diffraction method and was used to determine the crystal structure and phase purity of the prepared sample. The pattern was recorded on an EMPYREAN diffractometer system with  $\text{Cu K}\alpha$  radiation in the  $2\theta$  ( $\lambda = 1.5452\text{\AA}$ ). It was also characterized by the Fourier Transform Infrared technique using the Bruker equipment to help identify the various functional groups of the material.

## 2.4 Preparation of Dye Solution

Dye solutions of Colour Index Reactive Yellow 145 and Blue 194 solutions were laboratory prepared and used to assess the degradation efficiency of the MIL-53(Al) synthesized.

## 2.5 Photodegradation process

The dye degradation process was operated in a batch mode. An amount of the synthesized adsorbent [MIL-53(AL)] was dissolved in 25mL of the dye solution. This mixture was stirred continuously using the Stuart UC 121 magnetic stirrer. Samples were withdrawn from the reaction mixture at varying time differences of 30 mins, 60 mins, 90 mins, 120 mins, 150 mins, 180 mins, and 240 mins. It was then filtered and the absorbance measured at wavelength of 420 nm and 610 nm for color index Yellow 145 and color Blue 194 respectively. The final concentration was determined using the UV-Vis Spectrophotometer (Shimadzu, UV-160A).

## 2.6 Mineralization of Dyes

The chemical intermediates from the photodegradation process was analysed to identify the products of this process. After the photodegradation process 10ml of hexane was added to the mixture in a separator funnel. This was done to help remove any residual dye. It was then dried using the Rotary Evaporator and then with MgSO<sub>4</sub> to improve the drying process. The mixture was filtered and analyzed using the GC/MS

## 2.7 Percentage Degradation

The degradation efficiency of the dye concentrations was calculated using the efficiency relation equation below;

$$D\% = \left( \frac{C_o - C_t}{C_o} \right) \times 100 \quad (1)$$

where:

$D\%$  ----- percentage degradation of the dye concentration

$C_o$  ----- initial concentration of dyes in solution

$C_t$  ----- concentration of dyes in solution at the time (t)

## 2.8 Degradation Kinetics

To better understand the mechanism defining the degradation process, the kinetics of the process were examined.

The equation for the pseudo-first order Lagergren kinetic model is:

$$\frac{dq_t}{dt} = k_1 (Cq_e - q_t) \dots \dots \dots (2)$$

Integrating the equation above based on boundary conditions such as  $t = 0: q_t = 0$ , and  $t = t, q_t = q_t$  gives this linear equation;

$$\log \log (Cq_e - q_t) = \log q_e - \left( \frac{K_1}{2.303} \right) t \dots \dots \dots (3)$$

From equation (3) above, the amounts of dye degraded at equilibrium and at time  $t$  (mg/g) are denoted by  $Q_e$  and  $Q_t$  respectively. The contact time is denoted by the letter  $t$ . (min), The pseudo-first-order rate constant (/min) is denoted by  $K_1$ . This results in a straight-line plot of  $\log (Cq_e - q_t)$  against  $t$ , with  $\log (q_e)$  as slope and intercept equal  $\frac{K_1}{2.303}$ .

$$\frac{K_1}{2.303}$$

Considering the Pseudo second-order equation which is given below as;

$$\frac{dq_t}{dt} = k_2 (q_e - q_t)^2 \dots \dots \dots (4)$$

Using the same boundary conditions as in equation (2), the integration will give this equation:

$$\left( \frac{t}{q_t} \right) = \frac{1}{K_2 q_e^2} + \frac{1}{q_e} t \dots \dots \dots (5)$$

Where  $K_2$  is the second-order rate constant for the adsorption process

### 3.0 Results and Discussion

#### 3.1 X-Ray Diffraction Analysis

Figure 4 below shows the X-ray diffraction spectra of MIL-53(Al) which was synthesized and used in the degradation process.

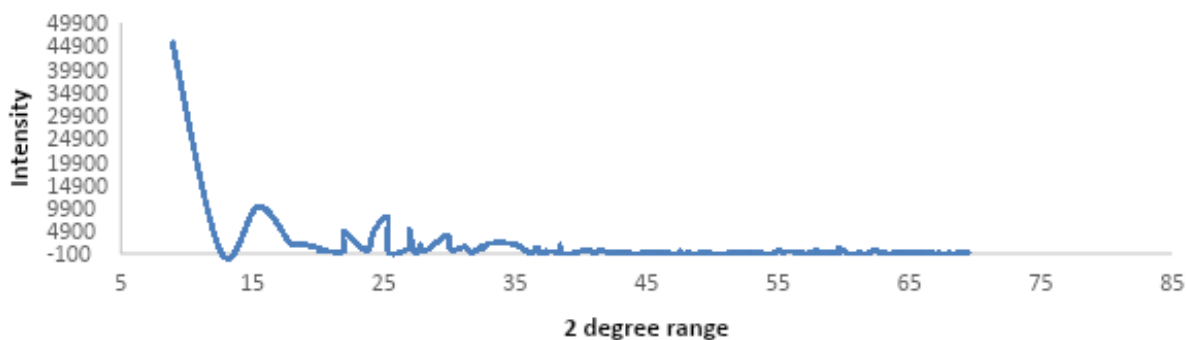


Figure 4: A graph showing the X- ray Diffraction pattern of MIL-53(Al)

The XRD of the material was similar to that synthesized by Rallipalli et.al. [51] and also Loiseau et.al.[50] where the broadness of the peak is recorded around an intensity of 9900. This is evident in the amorphous nature of the synthesized material.

### 3.2: Point of Zero Charge

The point of Zero charge of the synthesized material was performed using the combined procedure of Anang et.al. [51] and Jing et.al. [52] and presented as Figure 5. The starting pH was 3.1 and adjusted to 12.2 with the addition of NaCl. 0.2 g of MIL-53(Al) was added and kept for 24 hours. The relationship between the difference between the final and initial pH values ( $\Delta\text{pH} = (\text{pH}_f - \text{pH}_i)$ ) and  $\text{pH}_i$  was plotted, and the point of intersection of the curve with the abscissa yielded  $\text{pH}_{\text{PZC}}$

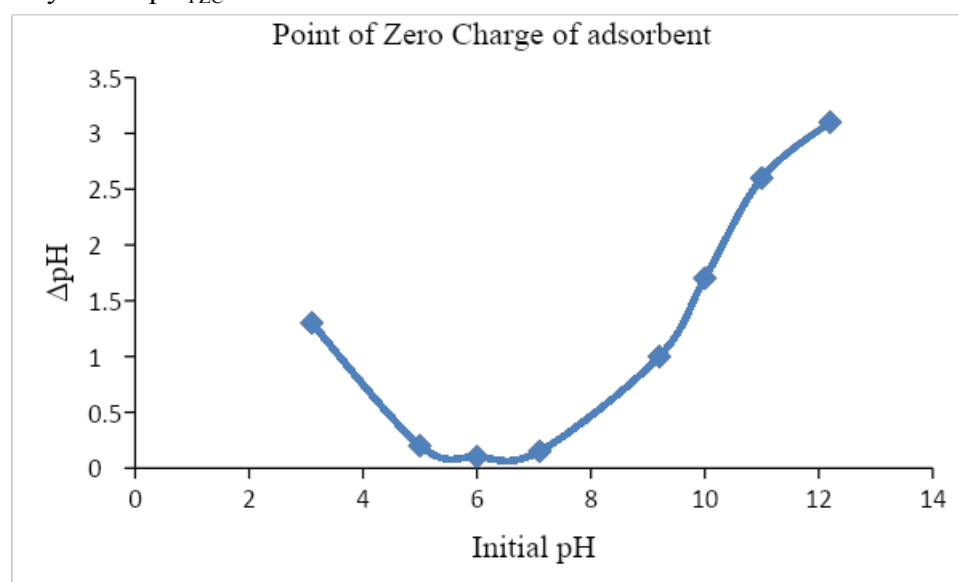


Figure 5: The Point of Zero charge of the synthesized MIL-53(Al)

### 3.2 Fourier Transform Infra-Red Analysis

The synthesized material was also characterized by the Fourier Transform Infrared technique using the Bruker equipment which exhibits vibration bands in the region 1,400–1,700  $\text{cm}^{-1}$  for the carboxylic functional group [53] as shown in Figure 6 below.

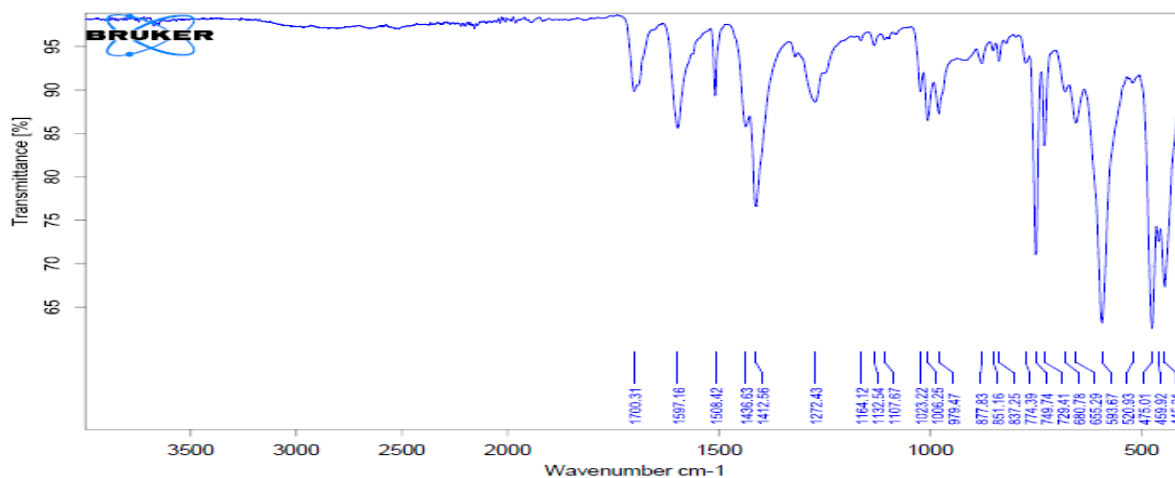


Figure 6: Fourier Transform infra-Red Spectra of MIL-53(Al)

Between 1500 – 1400 $\text{cm}^{-1}$  is the aromatics as well as the nitro compounds. Compounds such as alkanes and aromatic amines, esters and ethers were identified in the 1400 $\text{cm}^{-1}$  – 1200 $\text{cm}^{-1}$  range. The compounds also identified between the ranges of 910 - 665 $\text{cm}^{-1}$  represent the primary and secondary amines and further down with peaks at 800  $\text{cm}^{-1}$  to 600 $\text{cm}^{-1}$  are the single and triple bonds.

### 3.3 Percentage of Degradation

#### Effect of Change in Mass on adsorbent

The percentage degradation of the dyes was evaluated by using varying amounts (0.5 g, 1.0 g, and 1.5 g) of the adsorbent and the effect of the change in mass on the dye was assessed. The graph below shows the percentage reduction of color index Yellow 145 with time using MIL-53(Al) and labeled Figure 7

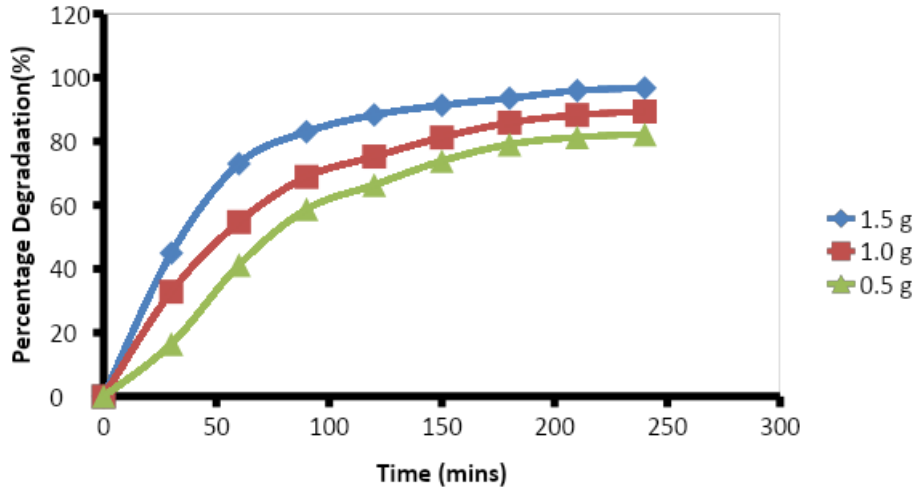


Figure 7: A Graph showing the percentage of degradation of Color Index Yellow 145

After 30 mins of the degradation process, the percentage reduction recorded was 44.92 %, 32.84 %, and 16.44 % for 1.5 g, 1.0 g, and 0.5 g masses of the adsorbent used respectively. This increased to 82.96 %, 68.84 %, and 58.68 % for the various masses after 90 mins. The percentage reduction of the dye concentration increased to 96.72 %, 89.34 %, and 82.22 % for 1.5 g, 1.0 g, and 0.5 g respectively after 240 mins of treatment. This trend does not vary much from the reduction process for color index Blue 194 as shown in Figure 8 below.

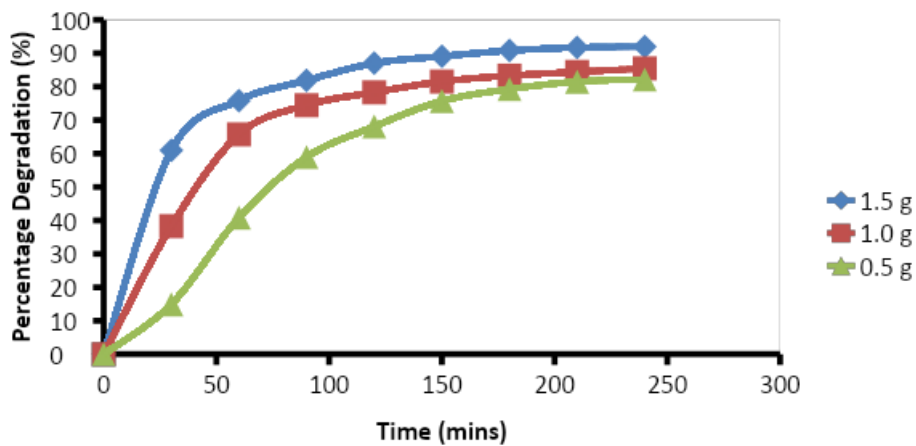


Figure 8: A Graph showing the percentage of degradation of Color Index Blue 194 using MIL-53(AI)

The initial 30 mins recorded a percentage reduction of 61.0 %, 38.3 %, and 14.92 % for the various masses of 1.5 g, 1.0 g, and 0.5 g respectively. This increased to 81.86 %, 74.45 %, and 58.94 % for 1.5 g, 1.0 g, and 0.5 g respectively after 90 mins with the highest been recorded after 240 mins showing values of 92.0 %, 85.47 %, and 82.2 % for the 1.5 g, 1.0 g, and 0.5 g masses respectively. From the above observations, it can be concluded that the percentage

reduction in the concentration of the dyes is mass-dependent. An increase in the amount of adsorbent causes an increase in the percentage reduction of the dye concentration.

### 3.4 Degradation Kinetics

Considering the Pseudo-first-order degradation kinetics from Figure 9, the  $R^2$  values were 0.9765, 0.9697, and 0.9853 for 1.5 g, 1.0 g, and 0.5 g respectively. The degradation constants  $K_1$  ( $\text{min}^{-1}$ ) were also 0.020727, 0.019806, and 0.008521 for the masses as described earlier

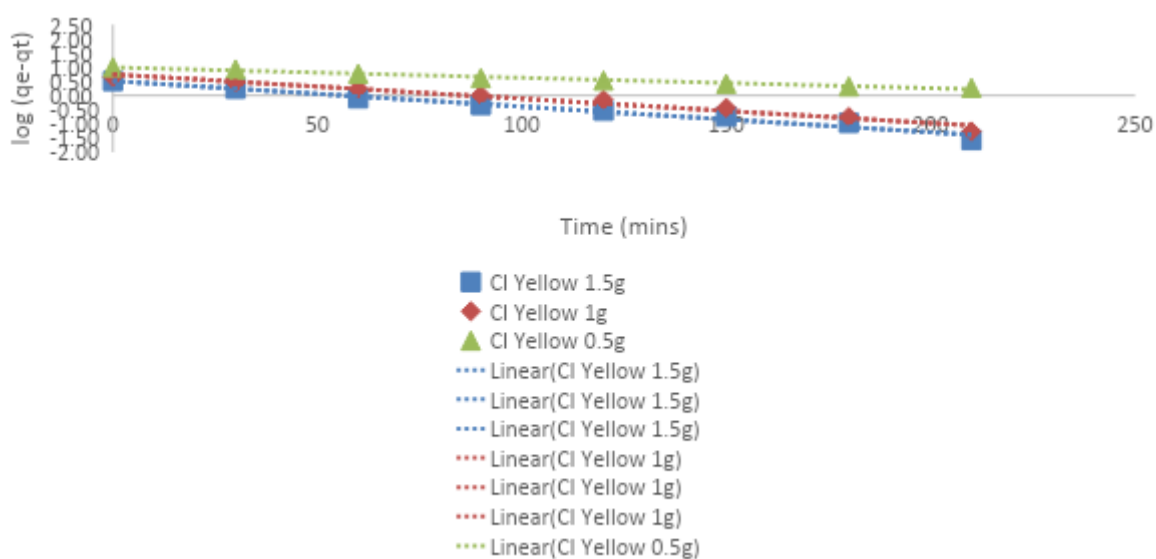


Figure 9: A Pseudo-first-order degradation graph of Color Index Yellow 145 using MIL-53(Al)

The amount of dye degraded at equilibrium ( $q_e$ ) mg/g recorded for the Pseudo first-order degradation process was 3.21803, 5.551368, and 9.788136. This implies the Pseudo first-order kinetics favors the 0.5 g degradation process.

The Pseudo-second-order degradation process, as shown in Figure 10, also recorded  $R^2$  values as 0.9966, 0.9956, and 0.8114 for 1.5 g, 1.0 g, and 0.5 g of MIL-53(Al).

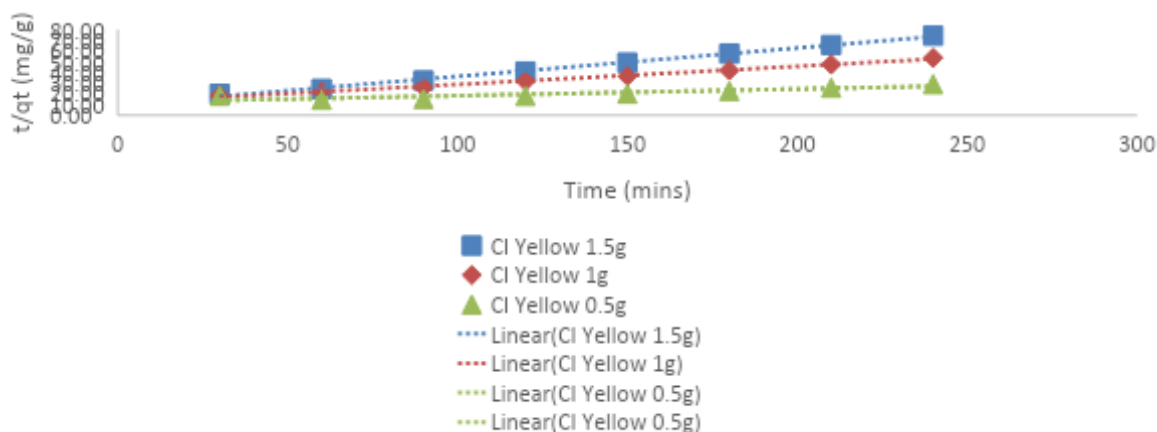


Figure 10: A Pseudo-second-order degradation graph of Color Index Yellow 145

The degradation constants  $k_2$  (g/mg-min) were also 3.762227, 5.882353, and 16 for the masses described above. The amounts of dye degraded at equilibrium are  $7.2225 \times 10^{-3}$ ,  $2.447 \times 10^{-3}$ , and  $3.23 \times 10^{-4}$  for the various masses respectively. This implies the Pseudo second-order degradation process for the color index Yellow 145 favors the 1.5 g mass of MIL-53(Al).

A summary of the kinetic data for the first and second-order degradation process is presented in Table 1

Table 1: A Table showing the parameters of the kinetics of Pseudo first and second-order degradation process for color Index 145 Yellow using MIL-53(Al)

	Pseudo-first-order degradation kinetics of Color Index 145 Yellow			Pseudo-second-order degradation kinetics of Color Index 145 Yellow			
	(1.5 g MIL-53)	(1.0g MIL-53)	(0.5g MIL-53)		(1.5g MIL-53)	(1.0g MIL-53)	(0.5g MIL-53)
$R^2$	0.9765	0.9697	0.9853	$R^2$	0.9966	0.9956	0.8114
$K_1(\text{min}^{-1})$	0.020727	0.019806	0.008521	$K_2(\text{g/mg-min})$	3.762227	5.882353	16
$q_e(\text{mg/g})$	3.218103	5.551368	9.788136	$q_e(\text{mg/g})$	0.007225	0.002447	0.000323
				$h(\text{mg/g-min})$	0.102271	0.084667	0.082631

The kinetics of the degradation process was also assessed for the color index Blue 194. As shown in Figure 11 and Table 2, the  $R^2$  values of 0.9789, 0.9954, 0.9787 for the 1.5 g, 1.0 g, and 0.5 g masses of the catalyst used with degradation constants ( $K_1 \text{min}^{-1}$ ) of 0.246421, 0.020266, and 0.008751 of the above masses respectively.

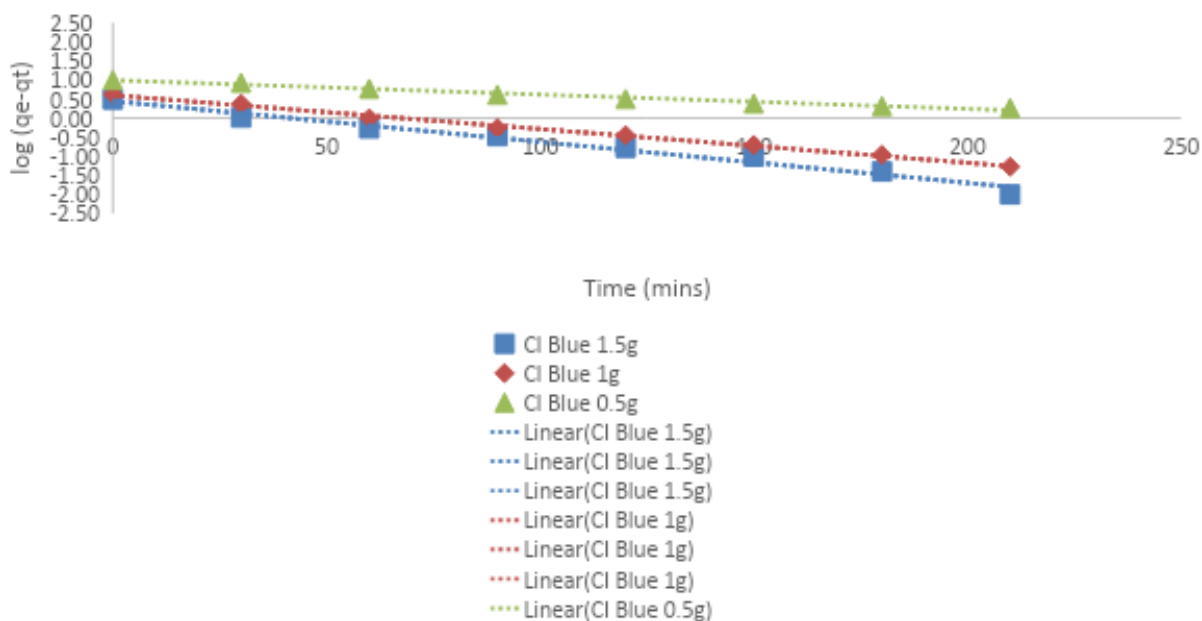


Figure 11: A Pseudo first-order degradation of Color Index Blue 194 using MIL-53(Al)

Table 2: A table showing the Parameters of the Pseudo-first and second-order degradation process of color index Blue 194 using MIL-53(Al)

	Pseudo-first-order degradation kinetics of Color Index 194 Blue			Pseudo-second-order degradation kinetics of Color Index Blue 194			
	(1.5 g MIL-53)	(1.0 g MIL-53)	C. I Blue 0.5 g		(1.5 g MIL-53)	(1.0 g MIL-53)	(0.5 g MIL-53)
R <sup>2</sup>	0.9789	0.9954	0.9787	R <sup>2</sup>	0.9998	0.9937	0.6885
K <sub>1</sub> (min <sup>-1</sup> )	0.246421	0.020266	0.008751	K <sub>2</sub> (g/mg-min)	3.324468	4.997501	17.54386
q <sub>e</sub> (mg/g)	2.797049	3.960044	9.835581	q <sub>e</sub> (mg/g)	0.01611	0.005468	0.000251
				h (mg/g-min)	0.178044	0.136571	0.077202

The amounts of dye degraded at equilibrium (q<sub>e</sub>) are 2.797049, 3.960044, and 9.835581 for masses of 1.5 g, 1.0 g, and 0.5 g catalysts respectively. It can be concluded that the degradation process for the color index Blue 194 favored the Pseudo-first-order for 1.0 g mass catalyst.

The Pseudo-second-order degradation kinetics of color index Blue 194 using MIL-53(Al) in Figure 12 also recorded R<sup>2</sup> values of 0.9998, 0.9937, and 0.6885 for the 1.5 g, 1.0 g, and 0.5 g mass catalysts

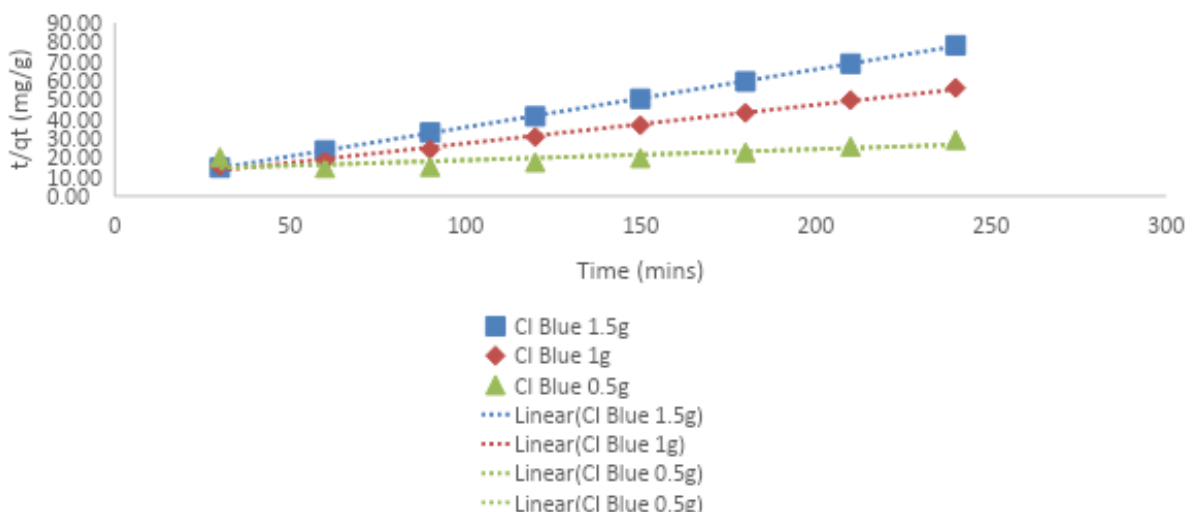


Figure 12: A Pseudo second-order degradation graph of color index Blue 194 using MIL-53(Al)

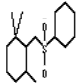
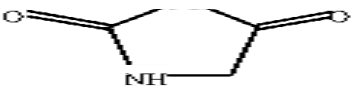
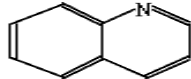
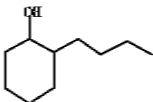
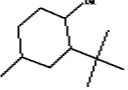
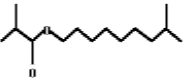
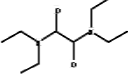
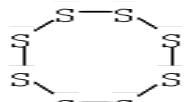
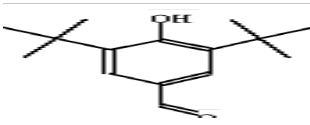
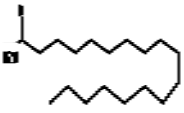
The degradation constants ( $k_2$  g/mg-min) were also 3.324468, 4.997501, and 17.54386 for the various masses above. The initial degradation rates are 0.178044, 0.136571, and 0.77202 respectively. The amounts of dye degraded at equilibrium are 0.01611, 0.005468, and 0.000251 for the masses considered. It can therefore be also concluded that the degradation process using a mass of 1.5 g favored the Pseudo-second-order kinetic process.

### 3.5 Photo-degraded Products

The extract from the degradation process was taken through several analytical process to help identify the chemical product obtained from the extract. First Hexane was added to the extract to help release the dye component which may interfere with the readings. This was performed using the separating funnel. After the extraction process the residue was discarded. The residual hexane was removed by evaporation using the Rotary evaporator. This drying process was further enhanced with  $MgSO_4$  which was latter filtered out/ The prepared samples were then analyzed using the GC/MS. The some of the intermediates obtained and their masses are presented in Table 3 below. The intermediates obtained from the photodegradation of Color Index 145 Yellow and Color Index 194 Blue after 90 mins of degradation was recorded

Table 3: A Table showing the some of the products obtained from the photodegradation of the dyes color index 145 Yellow and color index 194 Blue after 90 mins.

Colour Index 145 Yellow (90 mins) 1026.25 g/mol	Colour Index 194 Blue (90 mins) 1205.38 g/mol
--	--

 (2,6,6-Trimethylcyclohex-1-enylmethanesulfonyl)benzene (278.0 g/mol)	 2,4-imidazolidinedione (100.08 g/mol)
 Quinoline (129.16 g/mol)	 Cyclohexanol, 2-butyl-, (156.26 g/mol)
 phenol,2-(1,1-dimethylethyl)-4-methyl- (194.27 g/mol)	 Isodecyl methacrylate (226.36 g/mol)
 ethanediamide, tetraethyl- (200.28 g/mol)	 Cyclic octatomic sulphur (256.5 g/mol)
 3,5-di-tert-Butyl-4-hydroxybenzaldehyde (234.33 g/mol)	 9-Octadecenamide, (Z)- (281.5 g/mol)

It can be seen from Table 3 that, the reactive Azo dyes have been photodegraded into several intermediates, Reactive azo dye color index Yellow 145 with a molecular mass of 1026.25 g/mol has been degraded after 90 mins to obtain intermediates such as Quinoline (129.16 g/mol), phenol,2-(1,1-dimethylethyl)-4-methyl- (194.27 g/mol), ethanediamide, tetraethyl- (200.28 g/mol), and 3,5-di-tert-Butyl-4-hydroxybenzaldehyde (234.33 g/mol) and many others. Similarly, color index Blue 194, after 90 mins of the degradation process gave some chemical intermediates such as 2,4-imidazolidinedione (100.08 g/mol), Cyclohexanol-2-butyl (156.26 g/mol), Isodecylmethacrylate (226.36 g/mol), cyclic octatomic sulphur (256.5 g/mol) and 9-Octadecenamide (281.5 g/mol) and many others. It can therefore be concluded that the metal-organic framework MIL-53(Al) was able to effectively photodegrade the two reactive azo dyes.

#### 4.0 Conclusion

Metal-organic framework [MIL-53(Al)] was synthesized using a reviewed method and characterized with the X-ray diffraction and Fourier Infra-red techniques. It was used to degrade two reactive azo dyes namely, color index Yellow145 and color index Blue194 using sunlight. The percentage reduction of the dye concentration was very good as it was able to achieve about 90% for both dyes. This shows the effectiveness of the synthesized material. Mineralisation of the intermediates showed that the dyes have been broken down into smaller and simpler compounds. Compounds such as Quinoline and Isodecyl methacrylate were obtained from the degradation of both dyes after 90 mins of application. This confirms that the synthesized material was able to degrade the dyes efficiently. The research gave very interesting results that can be applied locally as a means of disposing of reactive azo dyes from the textile industry.

### Data Availability

Data for this research work are with the authors

### REFERENCES

1. Zerjava, G., et al., *Electron trapping energy states of TiO<sub>2</sub>–WO<sub>3</sub> composites and their influence on photocatalytic degradation of bisphenol A* Applied Catalysis B, 2017. **209**: p. 273.
2. Ali, I., M. Asim, and T. Khan, *Low cost adsorbents for the removal of organic pollutants from wastewater*. Journal of Environmental Management, 2012. **113**(30): p. 170-183.
3. Arslan, S., et al., *A Review of State-of-the-Art Technologies in Dye-Containing Wastewater Treatment—The Textile Industry Case*. [http://www.intechopen.com/books/textile-wastewater-treatment.](http://www.intechopen.com/books/textile-wastewater-treatment), 2016.

4. Wang, Z., et al., *Textile Dyeing Wastewater Treatment*. [www.intechopen.com/books/advances-in-treating-textile-effluent/textile-dyeing-wastewater-treatment](http://www.intechopen.com/books/advances-in-treating-textile-effluent/textile-dyeing-wastewater-treatment), 2011.
5. Pearce, C.I., J.R. Lloyd, and J.T. Guthrie, *The removal of color from textile wastewater using whole bacterial cells: a review*. *Dyes and Pigments*, 2003. **58**: p. 179-196.
6. Robinson, T., et al., *Remediation of dyes in textile effluent: a critical review on current treatment technologies with a proposed alternative*. *Bioresource Technology*, 2001. **77**(3): p. 247-255.
7. Chen, Q., et al., *Selective adsorption of cationic dyes by UiO-66-NH<sub>2</sub>*. *Applied Surface Science*, 2015. **327**: p. 77-85.
8. Ahmed, M.B., et al., *Progress in the biological and chemical treatment technologies for emerging contaminant removal from wastewater: A critical review*. *Journal of Hazardous Materials*, 2017. **323**(Part A): p. 274-298.
9. Hsu, Y.-C., C.-H. Yen, and H.-C. Huang, *Multistage treatment of high strength dye wastewater by coagulation and ozonation*. *Chemical Technology and Biotechnology*, 1998. **71**(1): p. 71-76.
10. Verma, A.K., R.R. Dash, and P. Bhunia, *A review on chemical coagulation/flocculation technologies for removal of colour from textile wastewaters*. *Journal of Environmental Management*, 2012. **93**(1): p. 154-168.
11. Noguera-Oviedo, K. and D.S. Aga, *Lessons learned from more than two decades of research on emerging contaminants in the environment*. *Journal of Hazardous Materials*, 2016. **316**: p. 242-251.
12. Woisetschläger, D., et al., *Electrochemical oxidation of wastewater – opportunities and drawbacks*. *Water and Science Technology*, 2013. **68**(5): p. 1173.
13. Gomez, E., et al., *Thermal plasma technology for the treatment of wastes: a critical review*. *Journal of Hazardous Materials*, 2009. **161**(2-3): p. 614.
14. Babuponnusami, A. and k. Muthukumar, *A review on Fenton and improvements to the Fenton process for wastewater treatment*. *Journal of Environmental Chemical Engineering*, 2014. **2**(1): p. 557.
15. Martínez, S.B., J. Pérez-Parra, and R. Suay, *Use of ozone in wastewater treatment to produce water suitable for irrigation*. *Water Resource Management*, 2011. **25**: p. 2109.
16. S., R.P., A.R. Abdul, and W.M. Ashri, *Review on the main advances in photo-Fenton oxidation system for recalcitrant wastewaters* *Journal of Industrial and Engineering Chemistry*, 2015. **21**: p. 53.
17. Kou, J., et al., *Selectivity enhancement in heterogeneous photocatalytic transformations*. *Chemical Reviews*, 2017. **117**(3): p. 1445.
18. Long, J.R. and O.M. Yaghi, *The pervasive chemistry of metal–organic frameworks*. *Chemical Society Reviews*, 2009. **38**: p. 1213-1214.
19. Zhou, H.C., J.R. Long, and O.M. Yaghi, *Introduction to Metal–Organic Frameworks*. *Chemical Reviews*, 2012. **112**: p. 673-674.
20. Lu, W., et al., *Tuning the structure and function of metal–organic frameworks via linker design*. *Chemical Society Reviews*, 2014. **43**: p. 5561-5593.
21. Eddaoudi, M., et al., *Systematic Design of Pore Size and Functionality in Isoreticular MOFs and Their Application in Methane Storage*. *Science*, 2002. **295**(469-72).
22. Murray, L.J., M. Dinca, and J.R. Long, *Hydrogen storage in metal–organic frameworks*. *Chemical Society Reviews*, 2009. **38**(5): p. 1294-1314.

23. D'Alessandro, D.M., B. Smit, and J.R. Long, *Carbon Dioxide Capture: Prospects for New Materials*. Angewandte Chemie International Edition, 2010. **49**(35): p. 6058-82.
24. Chen B, S. Xiang, and G. Qian, *Metal–Organic Frameworks with Functional Pores for Recognition of Small Molecules*. Accounts of Chemical Research, 2010. **43**: p. 1115-24.
25. Sumida, K., et al., *Carbon Dioxide Capture in Metal–Organic Frameworks*. Chemical Reviews, 2012. **112**(2): p. 724-781.
26. Li, J.-R., R.J. Kuppler, and H.-C. Zhou, *Selective gas adsorption and separation in metal–organic frameworks*. Chemical Society Reviews, 2009. **38**(5): p. 1477.
27. Bae, Y.-S. and R.Q. Snurr, *Development and Evaluation of Porous Materials for Carbon Dioxide Separation and Capture*. Angewandte Chemie International Edition, 2011. **50**(11): p. 586-596.
28. Farrusseng, D., S. Aguado, and C. Pinel, *Metal–Organic Frameworks: Opportunities for Catalysis*. Angewandte Chemie International Edition, 2009. **48**(13): p. 7502.
29. D., A.M., et al., *Luminescent metal–organic frameworks*. Chemical Society Reviews, 2009. **38**: p. 1330-52.
30. Kreno, L.E., et al., *Metal–Organic Framework Materials as Chemical Sensors*. Chemical Reviews, 2012. **112**: p. 1105-25.
31. Heine, J. and K. Muller-Buschbaum, *Engineering metal-based luminescence in coordination polymers and metal–organic frameworks*. Chemical Society Reviews, 2013. **42**(24): p. 9232-42.
32. Hu, Z., B.J. Deibert, and J. Li, *Luminescent metal–organic frameworks for chemical sensing and explosive detection*. Chemical Society Reviews 2014. **43**(16): p. 9815-9840.
33. Zhang, X., et al., *Coordination polymers for energy transfer: Preparations, properties, sensing applications, and perspectives*. Coordination Chemistry Reviews, 2015. **294**: p. 206-235.
34. Cui, Y., et al., *Luminescent Functional Metal–Organic Frameworks*. Chemical Reviews 2012. **112**(2): p. 1126-1162.
35. C-Y, S., National Communication, 2013. **4**(2717).
36. Du, J.J., et al., *New photocatalysts based on MIL-53 metal–organic frameworks for the decolorization of methylene blue dye*. Journal of Hazardous Materials 2011. **190**: p. 945-915.
37. Zhao, H., et al., *Construction of Pillared-Layer MOF as Efficient Visible-Light Photocatalysts for Aqueous Cr(VI) Reduction and Dye Degradation*. ACS Sustainable Chemistry & Engineering, 2017. **5**(5): p. 4449-4456.
38. Haque, E., et al., *Dichotomous adsorption behaviour of dyes on an amino-functionalised metal–organic framework, amino-MIL-101(Al)*. Journal of Material Chemistry, 2014. **2**: p. 193-203.
39. Kang, I.J., et al., *Chemical and Thermal Stability of Isotypic Metal–Organic Frameworks: Effect of Metal Ions*. Chemistry A European Journal, 2011. **17**(23): p. 6437-6442.
40. Low, J.J., et al., *Virtual High Throughput Screening Confirmed Experimentally: Porous Coordination Polymer Hydration*. Journal of the American Chemical Society, 2009. **131**(43): p. 15834-15842.
41. Fateeva, A., et al., *A Water-Stable Porphyrin-Based Metal–Organic Framework Active for Visible-Light Photocatalysis*. Angewandte Chemie International Edition, 2012. **51**(30): p. 7440-7444.

42. Gascon, J., et al., *Metal-Organic Framework Materials and Their Applications in Catalysis*. Journal of Catalysis, 2009. **261**: p. 75-87.
43. Couck, S., et al., *An Amine-Functionalized MIL-53 Metal–Organic Framework with Large Separation Power for CO<sub>2</sub> and CH<sub>4</sub>*. Journal of the American Chemical Society, 2009. **131**: p. 6326-6327.
44. Li, Z.H., et al., *The Metal–Organic Framework MIL-53(Al) Constructed from Multiple Metal Sources: Alumina, Aluminum Hydroxide, and Boehmite*. Chemistry A European Journal, 2015. **21**(18): p. 6913-6920.
45. Haque, E., et al., *Dichotomous adsorption behaviour of dyes on an amino-functionalised metal–organic framework, amino-MIL-101(Al)*. Journal of Material Chemistry, 2014. **2**: p. 193-203.
46. Yang, C.X., H.B. Ren, and X.P. Yan, *Fluorescent Metal–Organic Framework MIL-53(Al) for Highly Selective and Sensitive Detection of Fe<sup>3+</sup> in Aqueous Solution*. Analytical Chemistry, 2013. **85**(15): p. 7441-7446.
47. Du, J.J., et al., *New photocatalysts based on MIL-53 metal–organic frameworks for the decolorization of methylene blue dye*. Journal of Hazardous Materials, 2011. **190**: p. 945-951.
48. Lopez, H.A., et al., *Photochemical Response of Commercial MOFs: Al<sub>2</sub>(BDC)<sub>3</sub> and Its Use As Active Material in Photovoltaic Devices*. Journal of Physical Chemistry C, 2011. **115**(45): p. 22200-22206.
49. Yan, J., et al., *Metal-organic framework MIL-53(Al): synthesis, catalytic performance for the Friedel-Crafts acylation, and reaction mechanism*. Science China, 2015. **58**: p. 1544-1552.
50. Loiseau, T., et al., *A Rationale for the Large Breathing of the Porous Aluminum Terephthalate(MIL-53) Upon Hydration*. European Journal of Chemistry, 2004. **10**(6): p. 1373-1382.
51. Anang, M., R. Zuggle, and B. Sefa-Ntiri, *Assessing the Adsorptive and Photodegradative Efficiencies of ZSM-11 Synthesized from Rice Husk Ash*. Hindawi Journal of Chemistry, 2020. **Volume 2020, Article ID 6094126**,
52. Jing, H.-P., et al., *Photocatalytic degradation of methylene blue in ZIF-8*. Royal Society of Chemistry Advances, 2014. **4**: p. 54454-54462.
53. Loiseau, T., et al., *A Rationale for the Large Breathing of the Porous Aluminum Terephthalate (MIL-53) Upon Hydration*. Chemistry; A European Journal, 2004. **10**(6): p. 1373-1382.

#### COMPETING INTERESTS DISCLAIMER:

Authors have declared that no competing interests exist. The products used for this research are commonly and predominantly use products in our area of research and country. There is absolutely no conflict of interest between the authors and producers of the products because we do not intend to use these products as an avenue for any litigation but for the advancement of knowledge. Also, the research was not funded by the producing company rather it was funded by personal efforts of the authors.